Mitochondrial bioenergetics and structural network organization

Giovanni Bénard, Nadège Bellance, Dominic James, Philippe Parrone, Helder Fernandez, Thierry Letellier, Rodrigue Rossignol

Mitochondrial bioenergetics and structural network organization

Giovanni Benard[1], Nadège Bellance[1], Dominic James[2], Philippe Parrone[2], Helder Fernandez[3], Thierry Letellier[1] and Rodrigue Rossignol[1,*]

[1]Institut National de la Santé et de la Recherche Médicale (INSERM), U688 Physiopathologie Mitochondriale, Universite Victor Segalen-Bordeaux 2, 146 rue Leo-Saignat, F-33076 Bordeaux cedex, France
[2]Department of Cell Biology, University of Geneva, 30, Quai Ansermet 1211 Geneva 4, Switzerland
[3]Laboratoire de Biologie Moleculaire et de Sequencage, Institut de Biochimie et Genetique Cellulaires, UMR Universite Victor Segalen Bordeaux 2-CNRS 5095, box 64, 146 rue Leo Saignat, F-33076 Bordeaux Cedex, France
*Author for correspondence (e-mail: rossig@u-bordeaux2.fr)

Accepted 13 December 2006
Journal of Cell Science 120, 838-848 Published by The Company of Biologists 2007
doi:10.1242/jcs.03381

Summary

Mitochondria form a dynamic network, and it remains unclear how the alternate configurations interact with bioenergetics properties. The metabolic signals that link mitochondrial structure to its functional states have not been fully characterized. In this report, we analyze the bidirectional relationships between mitochondrial morphology and function in living human cells. First, we determined the effect of mitochondrial fission on energy production by using small interfering RNA (siRNA) targeting *DRP1*, which revealed the importance of membrane fluidity on the control of bioenergetics. Second, we followed the effect of rotenone, a specific inhibitor of respiratory chain complex I, which causes large structural perturbations, once a threshold was reached. Last, we followed changes in the mitochondrial network configuration in human cells that had been treated with modulators of oxidative phosphorylation, and in fibroblasts from two patients with mitochondrial disease where the respiratory rate, $\Delta\Psi$ and the generation of reactive oxygen species (ROS) were measured. Our data demonstrate that the relationship between mitochondrial network organization and bioenergetics is bidirectional, and we provide a model for analyzing the metabolic signals involved in this crosstalk.

Key words: Mitochondrial network, Fission, DRP1, Oxidative phosphorylation, Threshold effect

Introduction

Mitochondria were discovered in the late 19th century and were described as a collection of granules forming threads inside the cell (Benda, 1898). This view was confirmed by electron-microscopic observations of tissue, cultured cells and rat diaphragm muscle that revealed the existence of a mitochondrial network (mt-network) (Lewis and Lewis, 1914), also known as mitochondrial reticulum (Bakeeva et al., 1978; Poliakova et al., 1983). The central role of mitochondria in cellular energy production was demonstrated by the discovery of the respiratory chain and by the first investigations of oxidative phosphorylation (OXPHOS) (Chance and Williams, 1956; Mitchell, 1961). However, the importance of mt-network integrity was not evaluated in these important functional studies. Likewise, most bioenergetic studies were performed on isolated mitochondria from rat liver or muscle that do not maintain network continuity after fractionation procedures. By contrast, it has become clear that the mitochondrion exists in living human cells as a large tubular assembly, extending throughout the cytosol (Amchenkova et al., 1988) and in close contact with the nucleus, the endoplasmic reticulum (Szabadkai et al., 2003), the Golgi network and the cytoskeleton (Anesti and Scorrano, 2006). Mt-networks are very dynamic with typical conformations shifting between a fragmented state and a tubular continuum (De Vos et al., 2005; Margineantu et al., 2002). Currently, it is believed that the overall shape of the mitochondrion is controlled by the balance between fusion and fission events that are mediated by specific proteins (Hollenbeck and Saxton, 2005; Youle and Karbowski, 2005). However, it remains difficult to study the determinants of mitochondrial structural changes because organelle profiles are known to be impacted by a number of causes, ranging from physiology to pathology (Chan, 2006; Griparic and van der Bliek, 2001). Accordingly, mitochondria participate in a variety of cellular processes, indicating that the control of their dynamic shape is probably multifactorial and their impact on cell activity very diverse.

There is growing evidence of a close relationship between energy production and mt-network organization. For instance, the pioneering observations of Hackenbrock (Hackenbrock, 1966; Hackenbrock, 1968; Hackenbrock et al., 1971) revealed a rapid and reversible change of the mitochondrion from the so-called ‘orthodox’ to ‘condensed’ conformations upon activation of ATP synthesis. This was confirmed recently in living cells at the level of the mt-network with the thinning and branching of its tubules upon alternating cellular energy substrates from glycolytic to more oxidative forms (Jakobs et al., 2003; Meeusen et al., 2004; Rossignol et al., 2004). By contrast, fragmentation of the mt-network has been observed in fibroblasts from patients with alterations of mitochondrial energy production caused by genetic defects in respiratory-chain subunits (Capaldi et al., 2004; Koopman et al., 2005).

The opposite is also true, because pathological mutations in genes responsible for mitochondrial fusion or fission have been associated with alterations in the organization of the mt-network and with the inhibition of energy metabolism (Amati-Bonneau et al., 2005; Pich et al., 2005).

However, it is yet unclear whether the variable forms of the mt-networks are associated with different bioenergetic properties and whether alterations between configurations can be dictated by specific variations in mitochondrial energy production. The role of mitochondrial transmembrane electric potential ($\Delta\Psi$) is also uncertain because fragmentation of the mt-network was observed in situations where it was abolished (Ishihara et al., 2003; Legros et al., 2002; Lyamzaev et al., 2004; Meeusen et al., 2004; Meeusen and Nunnari, 2005), increased (De Vos et al., 2005; Gilkerson et al., 2000; Zoratti et al., 1982), or decreased (Brand et al., 1994; De Vos et al., 2005; Lyamzaev et al., 2004). Alternatively, the role of intracellular ATP concentration could be important because the depletion of NTPs by apyrase was observed to abolish fusion events, leading to fragmentation of the mt-network (Meeusen et al., 2004). In addition, variations of mitochondrial energy states are associated with variable levels of free radicals generated by the respiratory chain (Jezek and Hlavata, 2005) that have also been suggested as possible modulators of mt-network organization (Koopman et al., 2005; Pletjushkina et al., 2006). Hence, the relationships between mt-network organization and the state of energy production must be considered in a multi-parameter analysis where $\Delta\Psi$, respiration and reactive oxygen species (ROS) generation are measured.

Here, we analyzed the crosstalk between mitochondrial bioenergetics and organelle-network organization by combining three different approaches. First, we determined the bioenergetic features of HeLa cells impaired in mt-network fission using small interfering RNA (siRNA) targeting DRP1. Second, we characterized changes in mt-network organization following treatment of MRC5 fibroblasts with rotenone, a specific inhibitor of the respiratory chain complex I. Last, we followed changes of mt-network configuration in human primary cell lines treated with different modulators of OXPHOS and also in cells taken from two patients with mitochondrial diseases. On the basis of our data, we suggest a model where the flux-force relationship of mitochondrial OXPHOS can explain changes in mt-network organization.

Results

RNAi of DRP1 induces alterations in the mt-network organization of HeLa cells

HeLa cells in which DRP1 was silenced by RNAi, presented abnormal branching and excessive budding of the mt-network compared with wild-type cells, or in cells in which siRNA was not induced (Fig. 1A-C). Downregulation of DRP1 was verified by western blotting, showing a decrease in the levels of DRP1 expression (84±11% normalized to porin), compared with cells without siRNA induction (Fig. 1D). In these cells, we did not observe a change in the expression levels of porin or respiratory chain complex IV (subunit Va) (Fig. 1D). HeLa cells containing siRNA targeting DRP1 showed a slower rate of proliferation in glucose medium, in comparison with non-induced and control cells (Table 1). In glucose-deprived medium, these cells were unable to proliferate, and died after three days, in contrast with the controls. This suggests that in cells where DRP1 was downregulated the OXPHOS system is inefficient.

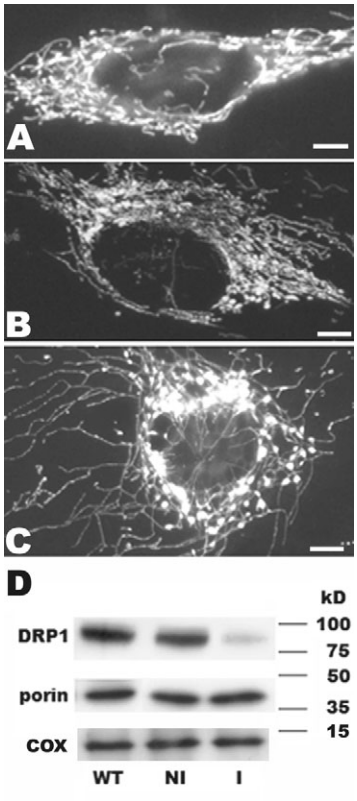

Fig. 1. Silencing of DRP1 in HeLa cells results in alterations of the mt-network morphology. (A-C) mt-network organization was observed in (A) wild-type HeLa cells, and (B) non-induced and (C) induced HeLa cells carrying the tet-inducible siRNA vector. Notice the budding of mt-network around the nucleus and the long, poorly ramified, tubules in C. Bars, 10 μm. (D) Western blots performed with 10 μg of cell-lysate proteins obtained from these cells.

Mitochondrial energy production is impaired in HeLa cells lacking DRP1

To look more closely at the effect DRP1-targeting RNAi has on the functioning of mitochondrial OXPHOS, we measured native cellular respiration as well as respiration in the presence of atractyloside (adenine-nucleotide-translocator inhibitor) and oligomycin (F_1F_0-ATP-synthase inhibitor) (Fig. 2A). The results show a significantly lower rate of endogenous respiration in cells where DRP1 levels were decreased, as compared to not-induced and wild-type cells ($P<0.05$). The respiratory rate measured in non-phosphorylating conditions, i.e. pseudo state 4 (Fig. 2B), was only slightly decreased, albeit significantly ($P<0.05$). As a consequence, the degree of endogenous coupling, represented by the ratio of the endogenous respiratory rate, to that measured in presence of atractyloside and oligomycin was lower ($P<0.05$) in cells containing siRNA targeting DRP1 (1.22±0.34) compared with not-induced (2.03±0.57) or wild-type (1.98±0.43) cells. This suggested that there is a reduced rate of mitochondrial ATP synthesis in cells containing siRNA targeting DRP1. Accordingly, measurement of the rate of mitochondrial ATP

Table 1. Bioenergetic parameters determined on entire cells or isolated mitochondria

	WT	NI	I
DT in galactose medium (hours)	41±5	47±6	–
DT in glucose medium (hours)	24±4	22±3	35±6*
Rate of mitochondrial ATP synthesis in permeabilized cells (nmol ATP/minute/10^6 cells)	16.08±4	12.96±3	5.1±1*
Isolated mitochondrial respiratory rate at state 4 (ng atom O/minute/mg)	8.05±0.61	9.17±0.34	2.87±0.14*
Isolated mitochondrial respiratory rate at state 3 (ng atom O/minute/mg)	21.87±0.11	23.12±0.54	5.44±0.30*

WT, wild-type; NI, non-induced; I, induced HeLa cells. Values are means ± s.d.
*P<0.05, statistically significant change compared with NI HeLa cells.

synthesis in permeabilized cells, using pyruvate-malate and ADP as substrates, revealed a strong deficiency (P<0.05) in HeLa cells containing siRNA targeting DRP1 compared with wild-type and not-induced cells (Fig. 2B). The respective rates of ATP synthesis are reported in Table 1.

Membrane properties and respiratory chain activity are impaired in mitochondria isolated from HeLa cells lacking DRP1

Isolated mitochondria from HeLa cells lacking DRP1 presented with a slower rate of state-4 and state-3 respirations (Table 1). We also observed a significant decrease in complex-IV activity when determined in situ on intact mitochondria respiring on ascorbate–*N,N,N′,N′*-tetramethyl-*p*-phenylenediamine (TMPD) (Fig. 3A). However, there was no difference in the ex-situ, activity of this complex, when measured spectrophotometrically, between cells lacking DRP1, not-induced cells or wild-type cells (Fig. 3B). The total amount of cytochrome *c* in the isolated mitochondria from these cells was also the same (Fig. 3C). However, we observed significant differences in the properties of mitochondrial membranes isolated from each cell type. Indeed, there was a large reduction of DPH anisotropy (increased membrane fluidity) in mitochondria isolated from HeLa cells containing siRNA targeting DRP1 (P<0.05) compared with not-induced and wild-type cells (Fig. 3D).

Inhibition of complex I by rotenone alters cellular metabolic capacity

After 4 hours of incubation with 1-5 ng/ml rotenone, we observed no significant change in cell viability (P<0.05) when compared with control cells (Fig. 4A); however, above 5 ng/ml, cell viability started to decrease rapidly. In those cells, we verified the inhibitory effect of rotenone on isolated activity of complex I, endogenous respiratory rate and cell proliferation (Fig. 4B). We found a rotenone-concentration-dependent decrease in complex I activity that was slightly attenuated at the level of cellular respiration and even more reduced at the level of cell proliferation. The representation of cell growth as a function of respiratory-rate inhibition revealed the existence of a threshold effect (Fig. 4C). This indicates that cell growth can remain quasi-normal even though mitochondrial respiration is inhibited up to 40%. Above that threshold, cell proliferation declines rapidly (Fig. 4C).

Inhibition of complex I by rotenone alters mt-network organization

Cells treated with 4-6 ng/ml rotenone for 4 hours showed a dramatic change in mt-network morphology characterized by

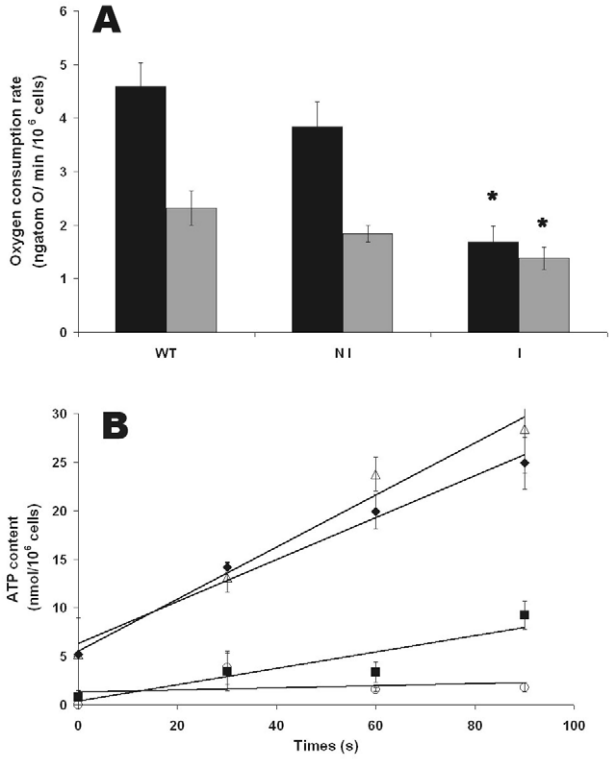

Fig. 2. Mitochondrial energetics is altered in HeLa cells where DRP1 levels were decreased. (A) Cellular endogenous respiration (black bars) was for wild-type (WT), not-induced (NI) or induced (I) HeLa cells cultured in galactose medium. The rate of respiration under non-phosphorylating conditions (gray bars) was obtained in cells incubated with oligomycin and atractyloside. (B) The rate of mitochondrial ATP synthesis was measured by bioluminometry for permeabilized cells with 10 mM pyruvate-malate and 2 mM ADP as substrates for wild-type (△), not-induced (◆) or induced (■) HeLa cells, and wild-type HeLa cells incubated with oligomycin and atractyloside (○). Results in A and B are given as the mean ± s.d., n=3; *P<0.05, statistically significant change compared with the NI cells.

vesicularization of the tubules and the appearance of numerous donut-like interdigitations (Fig. 4Dii). This was observed for a high proportion of cells (85±12%). Higher doses of rotenone, between 6 ng/ml and 10 ng/ml, induced mt-network fragmentation that appeared as a collection of stacked large rings (Fig. 4Diii). This configuration remained stable for 2-3 hours. In cells incubated with 10 ng/ml rotenone, the mt-network was fully fragmented and was constituted of numerous brightly fluorescent rings. However, at a rotenone level of

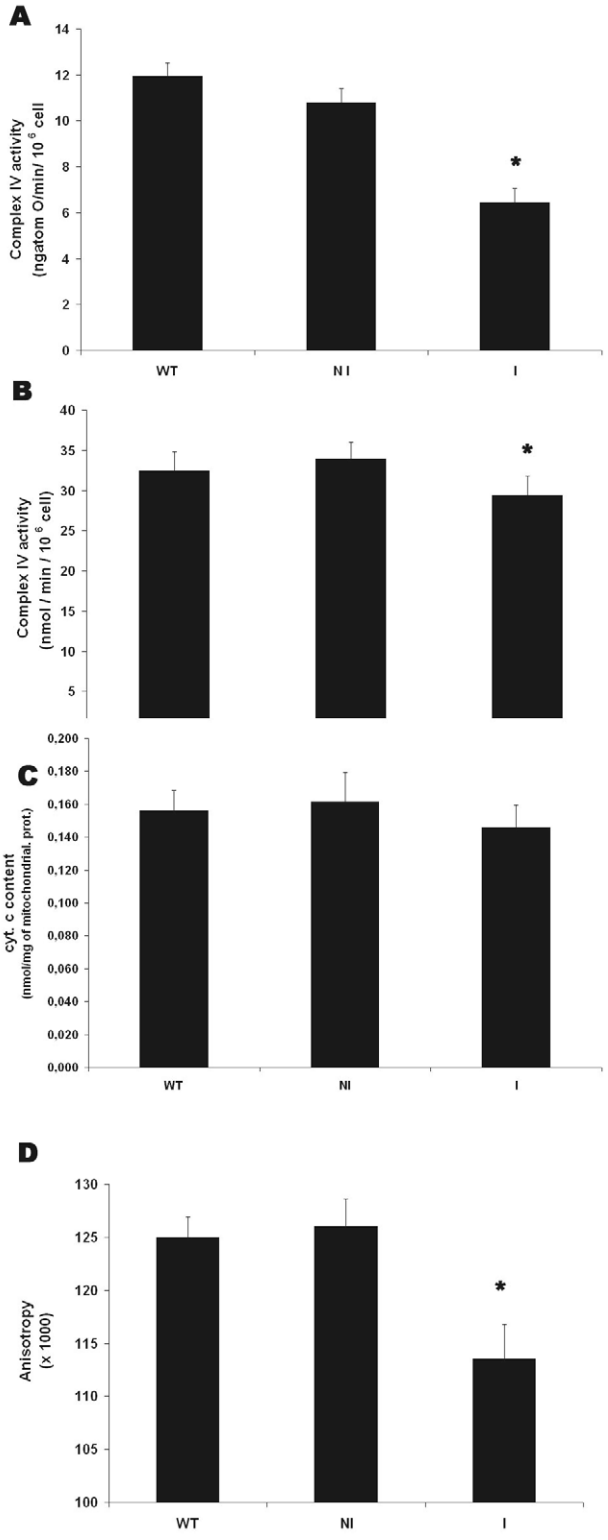

Fig. 3. Mitochondrial membrane fluidity is increased in HeLa cells with decreased DRP1 levels. (A) Mitochondrial respiratory rate measured in the presence of ascorbate-TMPD in wild-type (WT), not-induced (NI) or induced (I) HeLa cells. (B) Isolated activity of complex IV measured by spectrophotometry in the same cells. (C) The total content in cytochrome *c* determined by recording difference absorbance spectra. (D) DPH anisotropy measured in isolated mitochondria by fluorometry. The data indicate an increase in organelle membrane fluidity when DRP1 was silenced by RNAi. Results are given as the mean ± s.d., n=3; *P<0.05, statistically significant change compared with the NI cells.

above 10 ng/ml these vesicles were observed to disrupt, and the matrix GFP began to diffuse in the cytosol.

Inhibition of complex I by rotenone triggers a decrease in $\Delta\Psi$, an increase in matrix redox potential, and an increase in cytosolic ROS concentration

The effect of rotenone treatment (4 hours; variable concentration) on mitochondrial $\Delta\Psi$ was measured in MRC5 fibroblasts grown in galactose medium (Fig. 5A). We observed a reduction in $\Delta\Psi$, as indicated by a decrease in the JC1 red:green fluorescence ratio. However, it could not be inhibited more than 40% of the control value, even at rotenone concentrations >8 ng/ml, which were able to inhibit cell respiration to more than 85%. In our study, we also measured the effect of rotenone treatment on the steady-state level of cytosolic H_2O_2 by using the fluorescent probe H_2-DCFDA. However, it revealed no difference in ROS concentration in MRC5 fibroblasts treated with less than 9 ng/ml rotenone (Fig. 5B); above 9 ng/ml, the generation of radical species was increased significantly (P>0.05). We conducted the same analysis at the level of the mitochondrion, by using MitoSOX-Red, a fluorescent probe that reacts with mitochondrial superoxide. The results presented in Fig. 6B show a pattern of mt-ROS generation in response to the different OXPHOS effectors that is similar to that observed in the cytosol. Last of all, we measured the redox potential of the mitochondrial matrix by using ratiometric redox-sensitive GFP. It revealed alterations in matrix redox potential towards more reduced values in cell treated with rotenone (Fig. 5C).

'Flux-force-structure' model of mt-network organization

To elucidate the consequences of changes in bioenergetic parameters on mt-network organization, we used different effectors of OXPHOS, including carbonyl cyanide 3-chlorophenylhydrazone (CCCP, an uncoupler of OXPHOS), rotenone (complex-I inhibitor), atractyloside and oligomycin. On MRC5 cells grown in galactose medium and treated with these different compounds at various concentrations, we measured changes in the mitochondrial $\Delta\Psi$, the respiratory rate (JO_2), cytosolic ROS and mt-network organization. The results are presented in a flux-force-structure diagram (Fig. 6A), which shows that changes in $\Delta\Psi$ and JO_2 are not proportional. Treatment with CCCP induces an increase in cell respiration and a strong decrease in $\Delta\Psi$ (down to 30% of the control value) associated with fragmentation of the mt-network (Fig. 6Ab,c). However, no change in cytosolic or mitochondrial ROS concentration was observed compared with controls (Fig. 6Cb,c). Treatment with rotenone led to a strong and rapid decrease in JO_2 that was associated with a decrease in $\Delta\Psi$, which was down to 72% of control values. This was followed by progressive budding of the mt-network and the formation of ring-like structures (referred to as donuts), which turned into pure vesicles in cells treated with high doses of rotenone (Fig. 6Cd-f). A significant increase in ROS concentration was measured in cells treated with high doses of rotenone, but no change was observed at rotenone

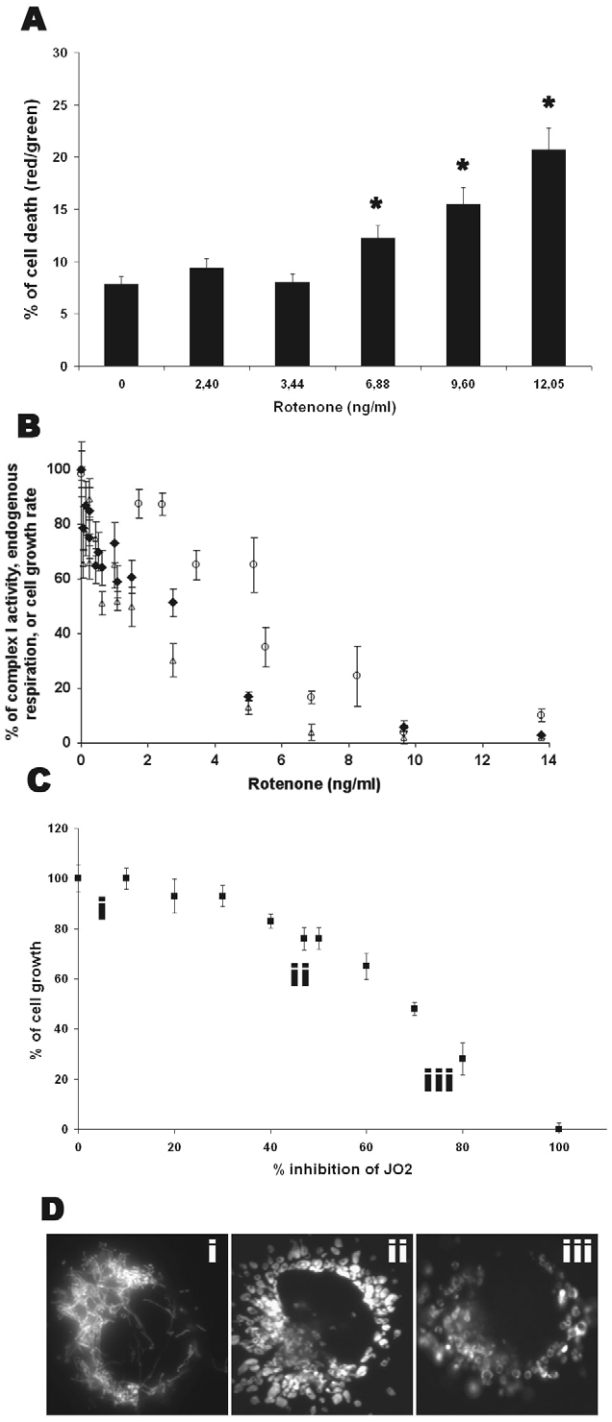

Fig. 4. Effect of rotenone treatment on MRC5 fibroblasts. (A) Cell viability in cells treated with different rotenone concentrations for 4 hours. (B) Rotenone titration curve of mitochondrial complex-I activity (△), cellular endogenous respiration (◆), and cell proliferation (○), expressed as percent of untreated control. (C) Inhibition of cell respiration and proliferation in galactose medium, expressed as percent of untreated control. Notice the threshold effect. (D) Morphological changes of the mt-network in cells treated with increasing rotenone concentrations. i, 0 ng/ml; ii, 3 ng/ml; iii, 6 ng/ml. Results are given as the mean ± s.d., n=3; *P<0.05, statistically significant change compared with the not induced.

concentrations below 12 ng/ml (d-f in Fig. 6A-C). Conversely, the treatment of MRC5 with oligomycin induced an increase in $\Delta\Psi$, associated with a decrease in cell respiration to levels comparable with pseudo-state-4 values. In this case, the mt-network became fragmented (Fig. 6B) and an augmented cytosolic ROS concentration was measured (Fig. 6B). Similar results were obtained with atractyloside (data not shown). In MRC5 cells grown in glucose medium, we found a slightly lower rate of endogenous respiration, a higher $\Delta\Psi$ and a slight decrease in ROS concentration compared with control cells grown in galactose medium (Fig. 6Aa′).

The mt-network of fibroblasts taken from either a patient carrying a complex-I defect (cell line B002, Fig. 6Ci) or a patient with multiple-respiratory-chain deficit (cell line F006, Fig. 6Cj), revealed important differences in mitochondrial morphology. The respiratory-chain-deficit cell line contained a mt-network that appeared more fragmented but was composed of numerous stacked vesicles that mimicked tubules. The complex-I-deficient cell line contained shorter mitochondrial tubules and many mitochondria with punctate dots. Both cell types were unable to grow in galactose medium and were deficient in their rate of respiration compared with controls. The values of endogenous respiratory rate and mitochondrial membrane potential measured in these cells were used to position these two cell lines on a diagram (Fig. 6A), which shows that the complex-I-deficient cell line has a slightly reduced $\Delta\Psi$ (83±04% of the control) and a more decreased respiration (48±06% of the control). The other cell line with the multiple-respiratory-chain deficit showed a more dramatic biochemical defect, with even smaller $\Delta\Psi$ (71±07% of the control) and respiration (22±03% of the control). Last, the induction of apoptosis in MRC5 cells with staurosporin led to the complete fragmentation of the mt-network (Fig. 6Ck). No change in ROS concentration was measured (Fig. 6B). Fine differences in mitochondrial ultrastructure can be observed, following the treatment with rotenone (Fig. 6C1) or CCCP (Fig. 6C2) compared with an untreated control (Fig. 6C3).

Discussion

The aim of this work was to study the interactions between mitochondrial energy production and the structural organization of the organelle. First, we analyzed cells in which the mt-network was deprived of the ability to fragment by suppressing DRP1 by RNAi. It resulted in extensive budding and elongation of the mt-nework, as described by other authors (Karbowski et al., 2004; Lee et al., 2004; Smirnova et al., 1998). This particular configuration was previously associated with a reduction in sensitivity to apoptosis inducers (Lee et al., 2004). In our study, it was associated with a strong inhibition of mitochondrial energy production, as demonstrated by the incapacity to grow in glucose-deprived medium (Robinson, 1996). It is important to notice that the mt-network of DRP1-depleted cells is different from that of control cells, even though their overall configuration appears mostly tubular. In DRP1-depleted cells, abnormal connectivity and a large number of budding areas were shown, which suggested a perturbation of mitochondrial dynamics. This was confirmed by the observation of increased mitochondrial membrane fluidity. The biochemical investigation of OXPHOS function in DRP1-depleted cells further revealed a reduction in the endogenous rate of coupled respiration, without a reduction of

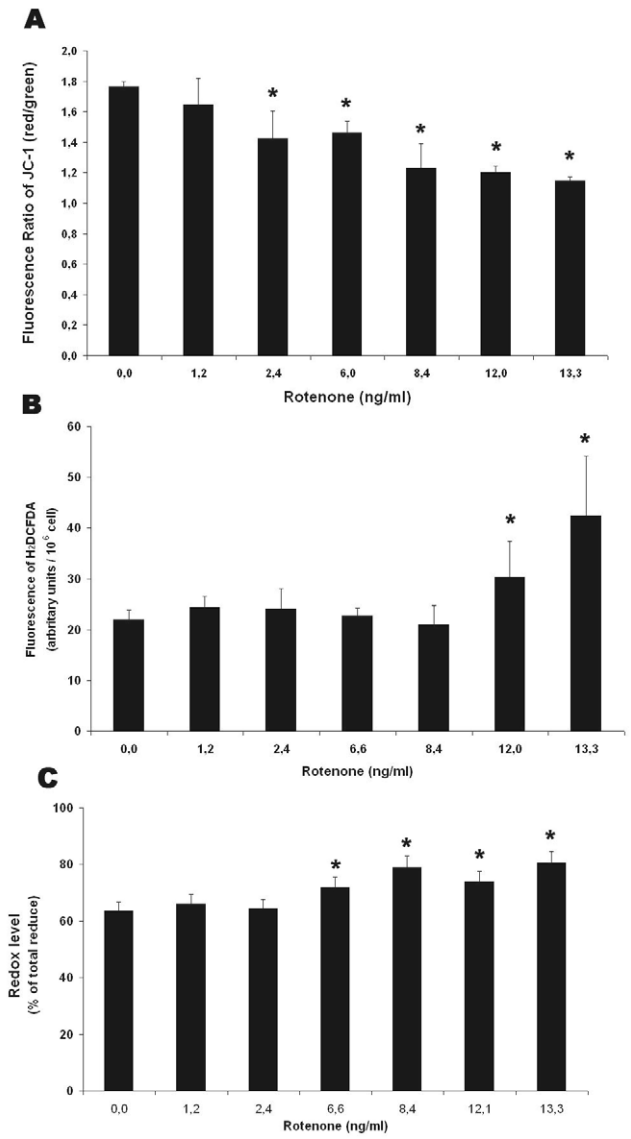

Fig. 5. Effect of rotenone treatment on mitochondrial ΨΔ, cytosolic ROS and matrix redox potential. (A) Determination of ΨΔ in MRC5 cells treated with increasing concentrations of rotenone, measured with the JC1 probe and expressed as the ratio of red to green fluorescence. (B) Determination of the cytosolic ROS concentration by fluorescence intensity of the H_2-DCFDA probe, expressed as the percentage of control value. Results are given as the mean ± s.d., n=3. (C) Measurement of the redox potential of the mitochondrial matrix in MRC5 cells treated with increasing rotenone concentrations, measured with redox-GFP and expressed as the percentage of the fluorescence intensity (emission ratio of 511 nm, excitation set at 400 nm and 480 nm) measured in control cells (not shown). *P<0.05, statistically significant change compared with the control.

that measured at pseudo-state-4. Accordingly, measurement of mitochondrial ADP phosphorylation in these cells when permeabilized with digitonin – where the delivery of substrates is not limiting – revealed a strong reduction of mitochondrial ATP synthesis. This suggests that a perturbation in the molecular machinery for ATP synthesis in HeLa cells where DRP1 levels are decreased, and can be explained by the observed perturbation of mitochondrial membrane fluidity. Accordingly, there was also a significant inhibition of complex-IV activity when measured in situ (polarography), compared with ex situ (spectrophotometry). These two assays reflect the membrane-dependent or membrane-independent activity of cytochrome *c* oxidase (COX), respectively. Previous studies have demonstrated a strong dependency of the F_1F_0-ATP-synthase activity on membrane fluidity (Aleardi et al., 2005; Ellis et al., 2005; Solaini et al., 1984) and a close association with cristae morphology (Paumard et al., 2002). Interestingly, recent analyses have indicated that DRP1 participates in the modeling of mitochondrial cristae, and its absence can disturb their organization (Germain et al., 2005). Here, we observed normal expression levels of COX and porin, suggesting that DRP1 suppression by RNAi had no impact on mitochondrial protein expression and insertion. It can be concluded from our data that mitochondrial fission is essential for normal OXPHOS function. Other groups reported the disruption of mitochondrial fission and observed the impairment of mitochondrial ATP production (Chen et al., 2005). It has also been demonstrated that mutations affecting the function of mitofusins are responsible for the Charcot-Marie-Tooth disease (Pich et al., 2005). Hence, it can be concluded that perturbation of mt-network dynamics, via fusion or fission disruption, is likely to induce the impairment of mitochondrial energy production.

In the second part of our work, we looked at the impact of OXPHOS inhibition on mt-network organization. It has previously been shown that cells taken from patients with a mitochondrial disease often present an alteration of mt-network morphology (Capaldi et al., 2004; Griparic and van der Bliek, 2001; Koopman et al., 2005). To mimick this situation, we used an inhibitor of respiratory chain complex I, at doses where it functions specifically (Barrientos and Moraes, 1999). Primary MRC5 human fibroblasts grown in galactose medium were treated for 4 hours with increasing doses of rotenone. This led to important changes in mt-network organization in cells treated with rotenone at 4-6 ng/ml. The tubules were no longer linear but circular, forming ring-like structures we called donuts. This phenomenon of circularization occurred at rotenone concentrations that inhibited the respiratory rate by about 40%, and when which cell proliferation just started to decline. This coincides with the threshold above which cells die rapidly when mitochondrial respiration is further inhibited. This threshold of cell resistance towards an OXPHOS defect is likely to be higher under physiological conditions, where glucose availability does not limit the production of ATP by glycolysis. Accordingly, we observed that, in a glucose medium, the rotenone concentration had to be increased to induce mt-network rearrangements (data not shown). The threshold for cell growth inhibition by rotenone was also higher in glucose medium compared with galactose medium (Barrientos and Moraes, 1999), suggesting that intracellular ATP concentration is an important parameter for the control of mt-network organization. These changes in mt-network morphology were rapid (within 4 hours), and the formation of donuts can be regarded as a direct consequence of impaired OXPHOS function or as a new, compensatory, mechanism (Rossignol et al., 2003). In cells treated with higher concentrations of rotenone (>6 ng/ml), the network fragmented further, and the donuts transformed into vesicles. This

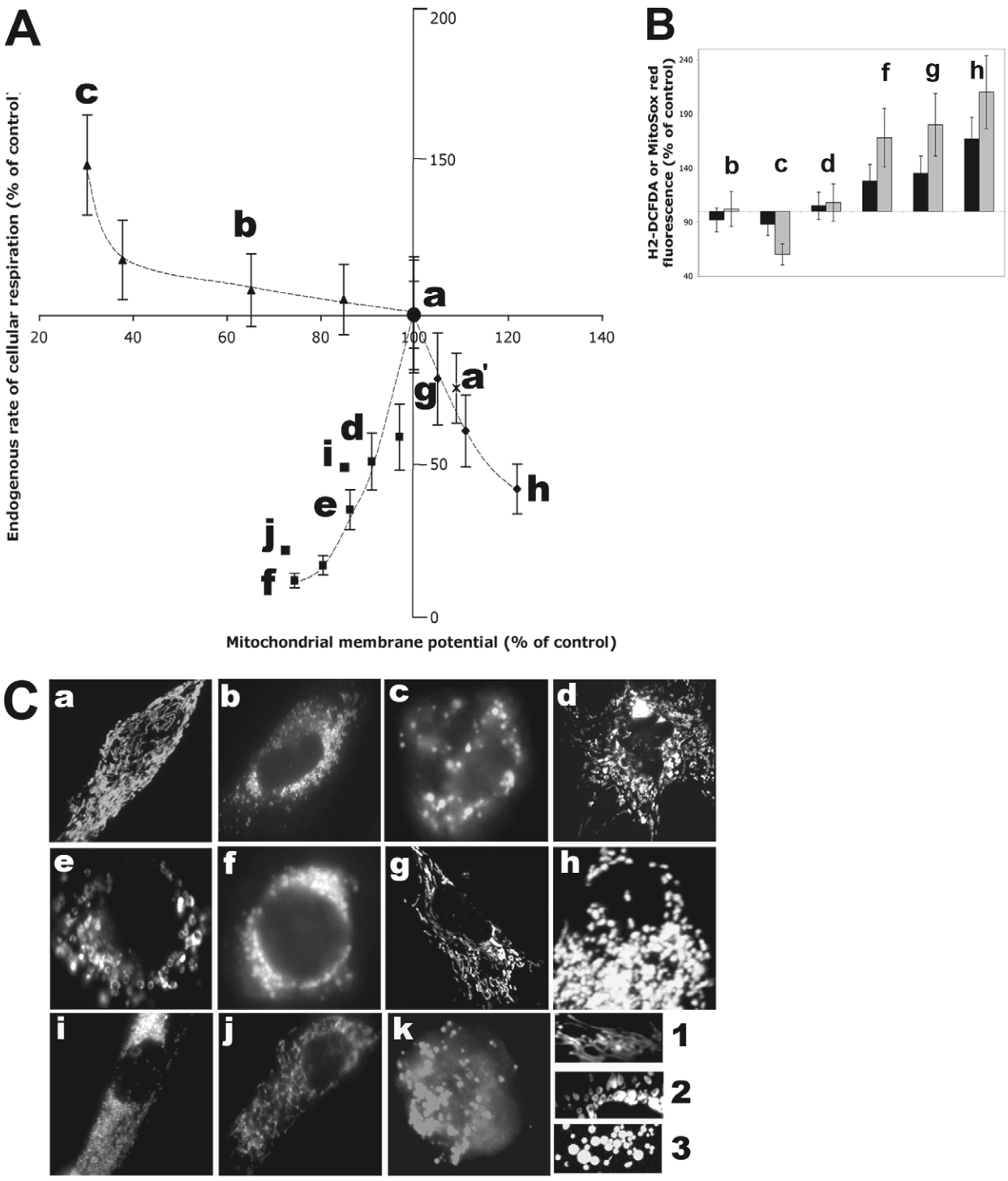

Fig. 6. Mitochondrial flux-force-structure diagram. (A-C) The energy state was modulated in living cells grown in a galactose medium (a), by three different means, which include: OXPHOS uncoupling with CCCP (b,c), respiratory chain inhibition with rotenone (d-f) and inhibition of mitochondrial ATP synthesis with oligomycin (g,h). All chemicals were added to the culture medium and incubated at 37°C. Rotenone was used for 4 hours at 2.4, 3.4 (d), 6.9 (e), 9.6 and 12 ng/ml (f). CCCP was used for 30 minutes at 5 and 10 μM (b), and 15 and 20 μM (c). Oligomycin was used at 0.1 and 0.2 ng/ml (g), and 0.5 ng/ml (h) for 3 hours. Staurosporin was used at 1 μM for 6 hours (k). Results for cells grown in glucose medium are also shown (a′). (A) Diagram showing the variation of mitochondrial respiration as a function of $\Delta\Psi$, expressed as a percentage of the control value and measured on MRC5 cells grown in galactose. (B) ROS steady-state level measured in the cytosol (black bars) or the mitochondrion (gray bars). Letters refer to the experimental conditions described in A. (C) mt-network organization observed in the above described situations labeled a-k. Also shown is the mt-network organization of cells taken from patients with (i) a severe complex-I defect and (j) multiple respiratory-chain deficiency. These cells lines are also positioned on the diagram shown in A, according to their bioenergetic coordinates. Fragmentation of the mt-network was also observed in MRC5 cells treated for 6 hours with staurosporin 1 μM (k). In addition, we discovered the details of mitochondrial ultrastructure in cells treated with rotenone (1) and CCCP (2), compared with the control (3).

fragmentation could reflect the induction of apoptosis, possibly triggered by the observed increase in ROS concentration, the drastic reduction of ATP concentration or the significant drop in $\Delta\Psi$. Thus, it cannot be excluded that fragmentation observed at these late time-points was the start of apoptotic cell degradation. Moreover, this phenomenon can occur rapidly, as observed for CV1 cells incubated for 45 minutes with rotenone (De Vos et al., 2005). However, in that study, the authors did not observe the self-circularization of the tubules, and the mt-network appeared fully fragmented. This may be explained by the high concentration of rotenone used in this study (25 μM) compared with the one we used (15 nM), as well as differences in cell type and species (simian versus human) or culture medium composition (glucose versus galactose). This could suggest that circularization is a sign of metabolic stress in living cells, whereas fragmentation indicates more an irreversible engagement to cell death.

In the third part of our study, we looked more closely at the relationships between $\Delta\Psi$, mitochondrial ATP synthesis and mt-network organization. Recent studies on the mechanisms of mitochondrial fusion, fission and its linkage to cytoskeletal elements have not evaluated the importance of bioenergetics on its regulation. Moreover, different studies on the implication of mitochondrial $\Delta\Psi$ in the control of mt-morphogenesis have been conflicting. For instance, it has been proposed that depolarization of $\Delta\Psi$ triggers reversible mt-network fragmentation. This has been observed in various cell types that were incubated in the presence of uncouplers such as CCCP, DNP or FCCP (Ishihara et al., 2003; Legros et al., 2002; Lyamzaev et al., 2004; Meeusen et al., 2004; Meeusen and Nunnari, 2005). Moreover, ρ^0 cells exhibit a lower $\Delta\Psi$ compared with clonal controls (Appleby et al., 1999; Loiseau et al., 2002) that also contain mitochondria and that form a fragmented network organization (Gilkerson et al., 2000). By contrast, the use of oligomycin, a specific inhibitor of the F_1F_0-ATP synthase or hydroxycinamic acid, an inhibitor of the phosphate carrier, also lead to mt-network fragmentation (De Vos et al., 2005). However, in this case there was hyperpolarization of $\Delta\Psi$, and a return to state-4 respiration (Chance and Williams, 1956; Zoratti et al., 1982). Furthermore, the addition of CCCP was seen to diminish the extent of fragmentation induced by oligomycin (De Vos et al., 2005), supporting the view that a high $\Delta\Psi$ triggers fragmentation. Accordingly, fragmentation of the mt-network is also induced by cyclosporine A, an inhibitor of the mPTP, which can cause an increase in $\Delta\Psi$ (Desagher and Martinou, 2000; Frank et al., 2001). Other studies have demonstrated that inhibition of respiratory chain complex I and complex III by various inhibitors can lead to mt-network fragmentation (De Vos et al., 2005; Lyamzaev et al., 2004). In this case, it is thought that fragmentation occurs through $\Delta\Psi$ depolarization (Brand et al., 1994). Furthermore, it has been shown that CCCP induces fragmentation more efficiently in the presence of a respiratory-chain inhibitor (De Vos et al., 2005). Hence, fragmentation of the mt-network appears to occur in situations where $\Delta\Psi$ is either abolished, increased or decreased. Moreover, experiments using uncoupler of OXPHOS often lacks simultaneous measurements of bioenergetic function and also ROS generation, which does not permit conclusions to be drawn about their impact on mitochondrial structure. These compounds have a very narrow window of active concentrations exemplified by the bell-shaped titration curves seen when observing mitochondrial respiration of living cells treated with these compounds (Desquiret et al., 2006). Another pitfall with previous studies concerns the use of tumor-derived cell lines grown in high-glucose medium that essentially derive ATP from glycolysis (Reitzer et al., 1979) and whose OXPHOS system is not very efficient (Pedersen, 1978; Rossignol et al., 2004). Worse yet, it is known that OXPHOS can work in a reverse mode, with the ATP produced by glycolysis being hydrolysed by F_1F_0-ATP synthase, causing $\Delta\Psi$ to be maintained without activity of the respiratory chain, as demonstrated in Rho^0 cells (Chevrollier et al., 2005; Loiseau et al., 2002). For these reasons, we used a model of non-tumor-derived primary fibroblasts grown in a culture medium that forced the the cells to derive energy actively by the OXPHOS-linked glutaminolytic pathway (Rossignol et al., 2004).

To elucidate the possible bioenergetic control of mt-network organization, we modulated OXPHOS function in three different ways that include (1) respiratory-chain inhibition with rotenone, (2) OXPHOS uncoupling with CCCP and (3) inhibition of mitochondrial ATP synthesis with oligomycin or atractyloside. We observed that even though mitochondrial respiration was fully inhibited, 60% of the endogenous mitochondrial membrane potential still remained. This indicates that a large fraction of $\Delta\Psi$ can be maintained by ions other than protons pumped by the respiratory chain. Similar observations were reported by other authors (Barrientos and Moraes, 1999; Loiseau et al., 2002). This compensatory phenomenon occured only in cells treated with rotenone, because the use of CCCP allowed a large part of the $\Delta\Psi$ (around 70%) to dissipate, suggesting that the majority was protonic in origin. Last, the addition of oligomycin induced an increase in $\Delta\Psi$ of about 20%, as compared with endogenous conditions, with a corresponding reduction in respiratory rate of about 50%. This indicates that in galactose medium, respiration was coupled and the cells were resting in a metabolic state between state 4 and state 3.

The diagram shown in Fig. 6 visualizes the effect of OXPHOS modulators on different bioenergetic parameters and their repercussion on mitochondrial morphology. For instance, rotenone treatment induced a small perturbation of $\Delta\Psi$, but caused a large reduction in respiratory rate and a decrease in consecutive ATP synthesis. This suggests that the circular structure of the mt-tubules depends more on ATP deprivation than on membrane depolarization. Moreover, it was suggested that ROS do not participate in this phenomenon because their production does not increase until high doses of rotenone were administered, conditions that induced complete mt-network fragmentation and loss of vesicles. In our study, the application of CCCP showed that $\Delta\Psi$ must be reduced to levels below 35% before the fragmentation process is observed to initiate. Separation of mt-vesicles was induced when the $\Delta\Psi$ value was below 60% of controls. However, this fragmentation might also be caused by the concomitant decrease in ATP synthesis triggered by uncoupling. Accordingly, in our study, the inhibition of ATP synthesis by oligomycin also triggered mt-network fragmentation. In this case, $\Delta\Psi$ is maintained, so that intracellular ATP deprivation is the best candidate for the promotion of mt-network metabolic fragmentation. This is consistent with observations of mt-fusion inhibition by apyrase, which can also lead to mt-network fragmentation

(Meeusen et al., 2004). The role of ROS in the fine-tuning of mt-network morphology is less evident. In our study, the increase in mitochondrial and cytosolic ROS concentration was only observed in cells treated with the highest concentrations of rotenone or oligomycin, and this was associated with rapid and massive fragmentation. This might suggest that changes in ATP concentration intervene early in the mediation of mt-network reorganization, whereas ROS might play a role the initiation of fragmentation under critical conditions. In our study, the two cell lines isolated from patients with a severe respiratory-chain deficiency showed abnormal organization of the mt-network. However, it is impossible to distinguish between the direct energy-dependent changes and the potential adaptative phenomena, which might explain why the respective position of these two cell lines on the flux-force-structure diagram cannot predict the shape of the organelle. Hence, more patient cell lines need to be analyzed to evaluate the importance of these adaptations.

Our observations raise important questions about the mechanisms controlling mt-network organization upon physiological changes, or even pathological alterations, of energy metabolism. For instance, fragmentation could result from the inhibition of fusion or the activation of fission, but these mechanisms are not clearly understood. Concerning fusion, it was demonstrated that fragmentation occurs when mitofusins are repressed (Chen et al., 2005). Recent developments indicate that Mfn2 GTPase activity is dependent of Bcl2 family members, so that the control mitochondrial morphogenesis might depend both on apoptosis and energy metabolism (Karbowski et al., 2006). Fragmentation can result from OPA1 processing in response to OXPHOS impairment (Ishihara et al., 2006). Again, this is evidence of a link between energetics and apoptosis, because OPA1 plays a role in controlling the availability of cytochrome *c* prior to its release (Cipolat et al., 2006; Frezza et al., 2006). Concerning mt-fission, changes in OXPHOS activity might interfere with the recruitment of DRP1 (Lee et al., 2004). Another important step in the control of mitochondrial morphogenesis exists at the level of mitochondrial lipid transformation (Choi et al., 2006; Steenbergen et al., 2005). To conclude, our results demonstrate that the relationship between mitochondrial form and function are bidirectional. They involve different properties of the mt-network, which can be regarded as a physical connector between energetics and apoptosis.

Materials and Methods

Chemicals

All chemicals used for mitochondrial preparations, enzymologic and polarographic studies were purchased from Sigma-Aldrich. Chemicals for western blot experiments were purchased from Biorad. Antibodies were obtained from Mitosciences or Santa Cruz Biotechnologies. Fluorescent probes were obtained from Invitrogen.

Cell types

HeLa and MRC5 cells were obtained from ATCC. The muscle fibroblasts were taken from two different patients with a mitochondrial disease and prepared in our laboratory, in collaboration with the Hospitals of Bordeaux (CHU Pellegrin – University Teaching Hospital, and Centre de Reference sur les maladies mitochondriales – Reference Centre for Mitochondrial Diseases). These cells were not transformed, and seeded on collagen-coated tissue culture dishes. The first cell line, B002 was generated from cells of a patient with a severe complex-I deficiency. The second cell line, F006, was generated from cells of a patient with multiple OXPHOS deficits caused by a deletion in mtDNA. Control fibroblasts were obtained from individuals originally screened for a mitochondrial disease that presented no defect in OXPHOS.

Cell culture conditions

The glucose medium consisted of high-glucose Dulbecco's modified Eagle's medium (DMEM) GIBCO containing 25 mM glucose, supplemented with 10% fetal calf serum (Hyclone), 100 U/ml penicilin, and 100 U/ml streptomycin. The galactose medium consisted of DMEM without glucose (GIBCO), supplemented with 10 mM galactose, 2 mM glutamine (4 mM final concentration), 10 mM Hepes, 1 mM sodium pyruvate, and 10% fetal calf serum-dialyzed (Hyclone). All cells were kept in a 10% CO_2 atmosphere at 37° C. Cell proliferation studies were carried out by plating 1.5×10^4 cells on 10-cm dishes (Corning) containing 20 ml of glucose- or galactose-medium. Cells were harvested by trypsinization and counted daily.

RNA interference

Downregulation of Drp1 levels in HeLa cells was achieved by RNA interference (RNAi) using a vector-based small-hairpin RNA (shRNA) approach (Brummelkamp et al., 2002). The target sequence was 5′-GCAGAAGAATGGGGTAAAT-3′ (NT 330-349, accession no. NM012063). The specificity of this sequence was confirmed by BLAST searches. Synthetic forward and reverse 64-nucleotide oligonucleotides (Microsynth, Switzerland) were designed, annealed and inserted into the *Bgl*II–*Hin*dIII sites of pSUPER-RETRO mammalian expression vector as previously described (Brummelkamp et al., 2002). The recombinant vectors expressed a 19-bp or 20-bp, 9-nucleotide stem-loop RNA structure specifically targeting different regions of the Drp1 transcript. To control for the potential side effects of transfecting cells with the pSUPER-RETRO vectors and expressing shRNA, all control cells were transfected with firefly luciferase-targeted shRNA-expressing pSUPER-RETRO vector (sequence 5′-CGTACGCGGAATACTTCGA-3′) as described in previously (Elbashir et al., 2001). The siRNA expression was induced in vivo by addition of 0.5 μg tetracycline for 24 hours. Tetracycline regulation in PSUPER-RETRO vectors is based on its binding to the Tet repressor and derepression of the promoter controlling expression of the gene of interest. In our case, the shRNA is expressed and cleaved into siRNA in the cell. These are small RNA fragments of 22-24 bp that recognise existing cellular RNA and bind to it forming a dsRNA, which activates RNAi. This leads to the destruction of the target mRNA, DRP1.

Cell transfection

Cells were plated 45 minutes before transfection and transfected using the calcium phosphate co-precipitation method (Jordan and Wurm, 2004). Twenty-four hours after transfection, the cells were washed once for 5 minutes with TBS and grown in fresh medium supplemented with 3 μg/ml puromycin (Calbiochem) for 24 hours to select for the transfected cells. The cultures were then washed with PBS and incubated in fresh growth medium until the start of the experiment. The maximal DRP1 downregulation was obtained 96 hours after transfection.

Cell viability

To determine the extent of cell death induced by rotenone treatment, we used the Live/Dead cell viability assay kit (Invitrogen), according the manufacturer's recommendations. The analysis was performed by fluorescence measurements on 96 well plates containing 10,000 cells per well. The results were expressed as the ratio of dead cells (red fluorescence) versus the total of living and dead cells (red and green fluorescence). For each condition a series of 12 different wells was analyzed, and the results expressed as the mean ± s.d.

Subcellular fractionation

Mitochondrial preparation was performed using digitonin, according the procedure described by Trounce et al. (Trounce et al., 1996), with modifications. Cells were grown in 150-mm^2 dishes, trypsinised (0.25%), centrifugated (1000 ***g***, 10 minutes) and resuspended in 1 ml of ice-cold buffer I (210 mM mannitol, 70 mM sucrose, 5 mM HEPES, 1 mM EGTA, 0.5% BSA). Digitonin was added to reach a final concentration of 1 mM, and cells were incubated 15 minutes on ice. Cell permeabilization was verified under the microscope using Trypan Blue. They were centrifugated (625 ***g***, 5 minutes) to remove digitonin, and the pellet was resuspended in 10 ml buffer I for homogenization in a glass potter on ice (40 gentle strikes). Again, cell membrane disruption was verified under the microscope. and cells were centrifuged (625 ***g***, 5 minutes) and the supernatant was kept on ice before another centrifugation step (10,000 ***g***, 20 minutes). The pellet of mitochondria was resuspended in buffer I. Typically, approximately 1 mg of mitochondrial proteins per 10^6 cells were recovered.

Measurement of mitochondrial membrane fluidity

Changes in the mitochondrial membrane fluidity were reported by measuring fluorescence anisotropy changes of the lipophilic probe 1,6-diphenyl-1,3,5-hexatriene (DPH). To incorporate the probe into the mitochondrial membrane, 0.2 mg/ml of mitochondria were incubated with DPH (4 μM final) for 20 minutes at 25°C in the dark. Fluorescence anisotropy (r) was measured at 30°C on a SAFAS genius spectro-fluoromiter, using excitation and emission wavelengths of 360 nm and 450 nm, respectively. The fluorescence anisotropy was calculated from emission intensities through a polarizer whose polarization axis was oriented parallel (I_{VV}) and perpendicular (I_{VH}) to the vertical polarization of excitation light. These

intensities were corrected against light diffusion measured on mitochondria without DPH as explained by Aleardi et al. (Aleardi et al., 2005).

Fluorescence microscopy

Cells were transfected with a mitochondrial targeted GFP as described by Rossignol et al. (Rossignol et al., 2004). The consecutive analysis of mitochondrial morphology was performed on living cells at 37°C, on a Nikon E 200 microscope, using a 60×, 1.4 N.A water-immersion objective. Series of images were acquired using a CoHu digital camera (1028×1022), driven by Visiolab 2000 Software. Excitation was set at 480 nm and emission recorded at 511 nm.

Measurement of mitochondrial transmembrane electric potential, matrix redox potential and ROS cytosolic or mitochondrial concentration

Cells were trypsinized, counted and incubated in presence of the various OXPHOS modulators in galactose medium. Different probes were used for measuring the relative mitochondrial membrane potential (JC1 and TMRM, Invitrogen). Changes in cytosolic ROS levels were monitored using the H_2-DCFDA probe (Invitrogen), whereas MitoSox red (Invitrogen) was used to detect mitochondrial ROS generation. These probes were added in the cell suspension, and incubated for 30 minutes at 37°C, according to the manufacturer's protocol. Cells were washed in PBS and fluorescence was measured at steady-state, in galactose medium with or without the desired reagents, on a spectrofluorometer (SAFAS). For the redox GFP, measurements were performed as described by Rossignol et al. (Rossignol et al., 2004).

Western blotting

Cell lysis was performed on ice using 0.4% lauryl-maltoside for 30 minutes. Samples were diluted into a SDS-PAGE tricine sample buffer (Bio-Rad) containing 2% β-mercaptoethanol, incubated for 30 minutes at 37°C and separated on a 10-22% SDS-PAGE gradient mini-gel (Bio-Rad) at 150 V. Proteins were transferred electrophoretically to 0.45-μm polyvinylidine difluoride (PVDF) membranes for 2 hours at 100 mA in CAPS buffer (3.3 g CAPS, 1.5 L 10% methanol, pH 11) on ice. Membranes were blocked overnight in 5% milk-PBS with 0.02% azide, and incubated for 3 hours with the primary antibodies purchased from Mitosciences. The anti-porin antibody was purchased from Calbiochem. After three washes with PBS-0.05% Tween 20, the membranes were incubated for 2 hours with horseradish-peroxidase-conjugated goat anti-mouse antibody (Bio-Rad) diluted in milk-PBS (5%). This secondary antibody was detected using the chemiluminescent ECL PlusTM reagent (Amersham). The signal was quantified by densitometric analysis using Image J (NIH) sofware.

Determination of complex-I activity

Cells grown in galactose medium were harvested and centrifuged. The pellet was frozen in liquid nitrogen and thawed at room temperature to allow membrane disruption. The activity of complex I was measured on 40 μg of proteins/ml in the presence of various concentrations of rotenone, by spectrophotometry as detailed in Benard et al. (Benard et al., 2006).

Respiration measurements

Mitochondrial oxygen consumption was monitored at 30°C in a 1-ml thermostatically controlled chamber equipped with a Clark oxygen electrode (Oxy 1, Hansatech). When human cells were analyzed, the respiratory buffer consisted of the galactose medium used for cell proliferation studies. For isolated mitochondria, the respiration buffer was prepared as follows: 75 mM mannitol, 25 mM sucrose, 10 mM KCl, 10 mM Tris Phosphate, 10 mM Tris-HCl pH 7.4, 50 μM EDTA and substrates (10 mM pyruvate, 10 mM malate). The mitochondrial concentration used for respiration measurements was 1 mg/ml, and state 3 was obtained by the addition of 2 mM ADP. Respiration rates were expressed in ng atom O/minute/mg protein.

Complex IV activity assays

Two methods were used to determine cytochrome *c* oxidase activity. The ex situ method was done spectrophotometrically by monitoring the oxidation of cytochrome *c* at 550 nm at 30°C. The exctinction coefficient was 18.5 mM^{-1} cm^{-1}. In the second method (in situ), we monitored cytochrome *c* oxidase activity by polarography using 3 mM ascorbate and 0.5 mM TMPD (as an electron donor system) with rotenone and antimycin.

ATP synthesis determination

Mitochondrial ATP synthesis was carried out on digitonin-permeabilized cells as described by Ouhabi et al. (Ouhabi et al., 1998). Steady-state ATP synthesis was initiated by adding 2 mM ADP and was recorded for 2 minutes as follows: every 30 seconds after ADP addition 10-μl aliquots were taken, quenched in 100 μl DMSO and diluted in 5 ml of ice-cold distilled water. For each collected sample, the quantity of ATP was measured using bioluminescence in a Luminoskan using the ATP monitoring reagent (ATP Bioluminescence Assay Kit HS II) from Boehringer Mannheim. Standardization was performed with known quantities of ATP provided with the kit (5, 10, 15, 20, 25 pmoles) and measured in parallel. The rate of ATP synthesis was calculated using linear regression. Rates were expressed in nmol ATP/minute/10^6 cells.

Determination of cytochrome *c* content

Cytochrome *c* content was determined by spectrophotometry on mitochondria isolated from HeLa cells (wild type, not-induced and induced) by performing redox difference cytochrome spectra as described in (Benard et al., 2006).

Statistical analysis

All the data presented in this study correspond to the mean value of *n* experiments ± s.e.m., with $n \geqslant 3$. Comparison of the data obtained from isolated muscle and liver mitochondria were performed with the Student's *t*-test, using Excel software (Microsoft). Two sets of data were considered statistically different when $P<0.05$.

We thank the INSERM, Université Victor Segalen Bordeaux 2, Association Française contre les Myopathies (AFM), Ligue contre le Cancer, Association Française contre les Maladies Mitochonriales (Ammi), and Région Aquitaine for financial support. We are also grateful to Jean-Claude Martinou for discussion, and to Devin Oglesbee for comments on our manuscript.

References

Aleardi, A. M., Benard, G., Augereau, O., Malgat, M., Talbot, J. C., Mazat, J. P., Letellier, T., Dachary-Prigent, J., Solaini, G. C. and Rossignol, R. (2005). Gradual alteration of mitochondrial structure and function by beta-amyloids: importance of membrane viscosity changes, energy deprivation, reactive oxygen species production, and cytochrome c release. *J. Bioenerg. Biomembr.* **37**, 207-225.

Amati-Bonneau, P., Guichet, A., Olichon, A., Chevrollier, A., Viala, F., Miot, S., Ayuso, C., Odent, S., Arrouet, C., Verny, C. et al. (2005). OPA1 R445H mutation in optic atrophy associated with sensorineural deafness. *Ann. Neurol.* **58**, 958-963.

Amchenkova, A. A., Bakeeva, L. E., Chentsov, Y. S., Skulachev, V. P. and Zorov, D. B. (1988). Coupling membranes as energy-transmitting cables. I. Filamentous mitochondria in fibroblasts and mitochondrial clusters in cardiomyocytes. *J. Cell Biol.* **107**, 481-495.

Anesti, V. and Scorrano, L. (2006). The relationship between mitochondrial shape and function and the cytoskeleton. *Biochim. Biophys. Acta* **1757**, 692-699.

Appleby, R. D., Porteous, W. K., Hughes, G., James, A. M., Shannon, D., Wei, Y. H. and Murphy, M. P. (1999). Quantitation and origin of the mitochondrial membrane potential in human cells lacking mitochondrial DNA. *Eur. J. Biochem.* **262**, 108-116.

Bakeeva, L. E., Chentsov Yu, S. and Skulachev, V. P. (1978). Mitochondrial framework (reticulum mitochondriale) in rat diaphragm muscle. *Biochim. Biophys. Acta* **501**, 349-369.

Barrientos, A. and Moraes, C. T. (1999). Titrating the effects of mitochondrial complex I impairment in the cell physiology. *J. Biol. Chem.* **274**, 16188-16197.

Benard, G., Faustin, B., Passerieux, E., Galinier, A., Rocher, C., Bellance, N., Delage, J. P., Casteilla, L., Letellier, T. and Rossignol, R. (2006). Physiological diversity of mitochondrial oxidative phosphorylation. *Am. J. Physiol. Cell Physiol.* **291**, C1172-C1182.

Benda, C. (1898). Ueber die Spermatogenese der Vertebraten und höherer Evertebraten, II. Theil: Die Histiogenese der Spermien. *Arch. Anat. Physiol.* **73**, 393-398.

Brand, M. D., Chien, L. F. and Diolez, P. (1994). Experimental discrimination between proton leak and redox slip during mitochondrial electron transport. *Biochem. J.* **297**, 27-29.

Brummelkamp, T. R., Bernards, R. and Agami, R. (2002). A system for stable expression of short interfering RNAs in mammalian cells. *Science* **296**, 550-553.

Capaldi, R. A., Murray, J., Byrne, L., Janes, M. S. and Marusich, M. F. (2004). Immunological approaches to the characterization and diagnosis of mitochondrial disease. *Mitochondrion* **4**, 417-426.

Chan, D. C. (2006). Mitochondria: dynamic organelles in disease, aging, and development. *Cell* **125**, 1241-1252.

Chance, B. and Williams, G. R. (1956). The respiratory chain and oxidative phophorylation. *Adv. Enzymol.* **17**, 65-134.

Chen, H., Chomyn, A. and Chan, D. C. (2005). Disruption of fusion results in mitochondrial heterogeneity and dysfunction. *J. Biol. Chem.* **280**, 26185-26192.

Chevrollier, A., Loiseau, D., Chabi, B., Renier, G., Douay, O., Malthiery, Y. and Stepien, G. (2005). ANT2 isoform required for cancer cell glycolysis. *J. Bioenerg. Biomembr.* **37**, 307-316.

Choi, S. Y., Huang, P., Jenkins, G. M., Chan, D. C., Schiller, J. and Frohman, M. A. (2006). A common lipid links Mfn-mediated mitochondrial fusion and SNARE-regulated exocytosis. *Nat. Cell Biol.* **8**, 1255-1262.

Cipolat, S., Rudka, T., Hartmann, D., Costa, V., Serneels, L., Craessaerts, K., Metzger, K., Frezza, C., Annaert, W., D'Adamio, L. et al. (2006). Mitochondrial rhomboid PARL regulates cytochrome c release during apoptosis via OPA1-dependent cristae remodeling. *Cell* **126**, 163-175.

De Vos, K. J., Allan, V. J., Grierson, A. J. and Sheetz, M. P. (2005). Mitochondrial function and actin regulate dynamin-related protein 1-dependent mitochondrial fission. *Curr. Biol.* **15**, 678-683.

Desagher, S. and Martinou, J. C. (2000). Mitochondria as the central control point of apoptosis. *Trends Cell Biol.* **10**, 369-377.
Desquiret, V., Loiseau, D., Jacques, C., Douay, O., Malthiery, Y., Ritz, P. and Roussel, D. (2006). Dinitrophenol-induced mitochondrial uncoupling in vivo triggers respiratory adaptation in HepG2 cells. *Biochim. Biophys. Acta* **1757**, 21-30.
Elbashir, S. M., Harborth, J., Lendeckel, W., Yalcin, A., Weber, K. and Tuschl, T. (2001). Duplexes of 21-nucleotide RNAs mediate RNA interference in cultured mammalian cells. *Nature* **411**, 494-498.
Ellis, C. E., Murphy, E. J., Mitchell, D. C., Golovko, M. Y., Scaglia, F., Barcelo-Coblijn, G. C. and Nussbaum, R. L. (2005). Mitochondrial lipid abnormality and electron transport chain impairment in mice lacking alpha-synuclein. *Mol. Cell. Biol.* **25**, 10190-10201.
Frank, S., Gaume, B., Bergmann-Leitner, E. S., Leitner, W. W., Robert, E. G., Catez, F., Smith, C. L. and Youle, R. J. (2001). The role of dynamin-related protein **1**, a mediator of mitochondrial fission, in apoptosis. *Dev. Cell* **1**, 515-525.
Frezza, C., Cipolat, S., Martins de Brito, O., Micaroni, M., Beznoussenko, G. V., Rudka, T., Bartoli, D., Polishuck, R. S., Danial, N. N., De Strooper, B. et al. (2006). OPA1 controls apoptotic cristae remodeling independently from mitochondrial fusion. *Cell* **126**, 177-189.
Germain, M., Mathai, J. P., McBride, H. M. and Shore, G. C. (2005). Endoplasmic reticulum BIK initiates DRP1-regulated remodelling of mitochondrial cristae during apoptosis. *EMBO J.* **24**, 1546-1556.
Gilkerson, R. W., Margineantu, D. H., Capaldi, R. A. and Selker, J. M. (2000). Mitochondrial DNA depletion causes morphological changes in the mitochondrial reticulum of cultured human cells. *FEBS Lett.* **474**, 1-4.
Griparic, L. and van der Bliek, A. M. (2001). The many shapes of mitochondrial membranes. *Traffic* **2**, 235-244.
Hackenbrock, C. R. (1966). Ultrastructural bases for metabolically linked mechanical activity in mitochondria. I. Reversible ultrastructural changes with change in metabolic steady state in isolated liver mitochondria. *J. Cell Biol.* **30**, 269-297.
Hackenbrock, C. R. (1968). Ultrastructural bases for metabolically linked mechanical activity in mitochondria. II. Electron transport-linked ultrastructural transformations in mitochondria. *J. Cell Biol.* **37**, 345-369.
Hackenbrock, C. R., Rehn, T. G., Weinbach, E. C. and Lemasters, J. J. (1971). Oxidative phosphorylation and ultrastructural transformation in mitochondria in the intact ascites tumor cell. *J. Cell Biol.* **51**, 123-137.
Hollenbeck, P. J. and Saxton, W. M. (2005). The axonal transport of mitochondria. *J. Cell Sci.* **118**, 5411-5419.
Ishihara, N., Jofuku, A., Eura, Y. and Mihara, K. (2003). Regulation of mitochondrial morphology by membrane potential, and DRP1-dependent division and FZO1-dependent fusion reaction in mammalian cells. *Biochem. Biophys. Res. Commun.* **301**, 891-898.
Ishihara, N., Fujita, Y., Oka, T. and Mihara, K. (2006). Regulation of mitochondrial morphology through proteolytic cleavage of OPA1. *EMBO J.* **25**, 2966-2977.
Jakobs, S., Martini, N., Schauss, A. C., Egner, A., Westermann, B. and Hell, S. W. (2003). Spatial and temporal dynamics of budding yeast mitochondria lacking the division component Fis1p. *J. Cell Sci.* **116**, 2005-2014.
Jezek, P. and Hlavata, L. (2005). Mitochondria in homeostasis of reactive oxygen species in cell, tissues, and organism. *Int. J. Biochem. Cell Biol.* **37**, 2478-2503.
Jordan, M. and Wurm, F. (2004). Transfection of adherent and suspended cells by calcium phosphate. *Methods* **33**, 136-143.
Karbowski, M., Arnoult, D., Chen, H., Chan, D. C., Smith, C. L. and Youle, R. J. (2004). Quantitation of mitochondrial dynamics by photolabeling of individual organelles shows that mitochondrial fusion is blocked during the Bax activation phase of apoptosis. *J. Cell Biol.* **164**, 493-499.
Karbowski, M., Norris, K. L., Cleland, M. M., Jeong, S.-Y. and Youle, R. J. (2006). Role of BAX and BAK in mitochondrial morphogenesis. *Nature* **443**, 658-662.
Koopman, W. J., Visch, H. J., Verkaart, S., van den Heuvel, L. W., Smeitink, J. A. and Willems, P. H. (2005). Mitochondrial network complexity and pathological decrease in complex I activity are tightly correlated in isolated human complex I deficiency. *Am. J. Physiol. Cell Physiol.* **289**, C881-C890.
Lee, Y. J., Jeong, S. Y., Karbowski, M., Smith, C. L. and Youle, R. J. (2004). Roles of the mammalian mitochondrial fission and fusion mediators Fis1, Drp1, and Opa1 in apoptosis. *Mol. Biol. Cell* **15**, 5001-5011.
Legros, F., Lombes, A., Frachon, P. and Rojo, M. (2002). Mitochondrial fusion in human cells is efficient, requires the inner membrane potential, and is mediated by mitofusins. *Mol. Biol. Cell* **13**, 4343-4354.
Loiseau, D., Chevrollier, A., Douay, O., Vavasseur, F., Renier, G., Reynier, P., Malthiery, Y. and Stepien, G. (2002). Oxygen consumption and expression of the adenine nucleotide translocator in cells lacking mitochondrial DNA. *Exp. Cell Res.* **278**, 12-18.
Lyamzaev, K. G., Pletjushkina, O. Y., Saprunova, V. B., Bakeeva, L. E., Chernyak, B. V. and Skulachev, V. P. (2004). Selective elimination of mitochondria from living cells induced by inhibitors of bioenergetic functions. *Biochem. Soc. Trans.* **32**, 1070-1071.
Margineantu, D., Cox, W., Sundell, L., Sherwood, S., Beechen, J. and Capaldi, R. (2002). Cell cycle dependent morphology changes and associated mitochondrial DNA redistribution in mitochondria of human cell lines. *Mitochondrion* **1**, 397-478.
Meeusen, S. L. and Nunnari, J. (2005). How mitochondria fuse. *Curr. Opin. Cell Biol.* **17**, 389-394.
Meeusen, S., McCaffery, J. M. and Nunnari, J. (2004). Mitochondrial fusion intermediates revealed in vitro. *Science* **305**, 1747-1752.
Mitchell, P. (1961). Coupling of phosphorylation to electron and hydrogen transfert by a chemi-osmotic type of mechanism. *Nature* **191**, 144-148.
Ouhabi, R., Boue-Grabot, M. and Mazat, J. P. (1998). Mitochondrial ATP synthesis in permeabilized cells: assessment of the ATP/O values in situ. *Anal. Biochem.* **263**, 169-175.
Paumard, P., Vaillier, J., Coulary, B., Schaeffer, J., Soubannier, V., Mueller, D. M., Brethes, D., di Rago, J. P. and Velours, J. (2002). The ATP synthase is involved in generating mitochondrial cristae morphology. *EMBO J.* **21**, 221-230.
Pedersen, P. L. (1978). Tumor mitochondria and the bioenergetic of cancer cells. *Prog. Exp. Tumor Res.* **22**, 190-274.
Pich, S., Bach, D., Briones, P., Liesa, M., Camps, M., Testar, X., Palacin, M. and Zorzano, A. (2005). The Charcot-Marie-Tooth type 2A gene product, Mfn2, up-regulates fuel oxidation through expression of OXPHOS system. *Hum. Mol. Genet.* **14**, 1405-1415.
Pletjushkina, O. Y., Lyamzaev, K. G., Popova, E. N., Nepryakhina, O. K., Ivanova, O. Y., Domnina, L. V., Chernyak, B. V. and Skulachev, V. P. (2006). Effect of oxidative stress on dynamics of mitochondrial reticulum. *Biochim. Biophys. Acta* **1757**, 518-524.
Poliakova, I. A., Zorov, D. B. and Leikina, M. I. (1983). Polarographic study of cell respiration in a tissue culture. *Tsitologiia* **25**, 162-167.
Reitzer, L., Wice, B. and Kennel, D. (1979). Evidence that glutamine, not sugar, is the major energy source for cultured Hela cells. *J. Biol. Chem.* **254**, 2669-2676.
Robinson, B. (1996). use of fibroblast and lymphoblast cultures for detection of respiratory chain defects. *Meth. Enzymol.* **264**, 455-464.
Rossignol, R., Faustin, B., Rocher, C., Malgat, M., Mazat, J. P. and Letellier, T. (2003). Mitochondrial threshold effects. *Biochem. J.* **370**, 751-762.
Rossignol, R., Gilkerson, R., Aggeler, R., Yamagata, K., Remington, S. J. and Capaldi, R. A. (2004). Energy substrate modulates mitochondrial structure and oxidative capacity in cancer cells. *Cancer Res.* **64**, 985-993.
Smirnova, E., Shurland, D. L., Ryazantsev, S. N. and van der Bliek, A. M. (1998). A human dynamin-related protein controls the distribution of mitochondria. *J. Cell Biol.* **143**, 351-358.
Solaini, G., Baracca, A., Parenti Castelli, G. and Lenaz, G. (1984). Temperature dependence of mitochondrial oligomycin-sensitive proton transport ATPase. *J. Bioenerg. Biomembr.* **16**, 391-406.
Steenbergen, R., Nanowski, T. S., Beigneux, A., Kulinski, A., Young, S. G. and Vance, J. E. (2005). Disruption of the phosphatidylserine decarboxylase gene in mice causes embryonic lethality and mitochondrial defects. *J. Biol. Chem.* **280**, 40032-40040.
Szabadkai, G., Simoni, A. M. and Rizzuto, R. (2003). Mitochondrial Ca2+ uptake requires sustained Ca2+ release from the endoplasmic reticulum. *J. Biol. Chem.* **278**, 15153-15161.
Trounce, I. A., Kim, Y. L., Jun, A. S. and Wallace, D. C. (1996). Assessment of mitochondrial oxidative phosphorylation in patient muscle biopsies, lymphoblasts, and transmitochondrial cell lines. *Meth. Enzymol.* **264**, 484-509.
Youle, R. J. and Karbowski, M. (2005). Mitochondrial fission in apoptosis. *Nat. Rev. Mol. Cell Biol.* **6**, 657-663.
Zoratti, M., Pietrobon, D. and Azzone, G. F. (1982). On the relationship between rate of ATP synthesis and H+ electrochemical gradient in rat-liver mitochondria. *Eur. J. Biochem.* **126**, 443-451.